Chemical Engineering Journal 162 (2010) 208–216

Contents lists available at ScienceDirect

Chemical Engineering Journal

journal homepage: www.elsevier.com/locate/cej

A CFD-based simulation study of a large scale flocculation tank for potable water treatment

K. Samaras, A. Zouboulis, T. Karapantsios, M. Kostoglou*

Division of Chemical Technology, Department of Chemistry, Aristotle University of Thessaloniki, University Box 116, 541 24 Thessaloniki, Greece

ARTICLE INFO

Article history:
Received 12 October 2009
Received in revised form 12 May 2010
Accepted 15 May 2010

Keywords:
Flocculation
Water refinery
Mathematical modeling
Sludge recirculation

ABSTRACT

A methodology is developed for simulating the operation of flocculation tanks for potable water treatment in the presence of very low solids concentration. The main effort of the simulation is devoted to the detailed representation of the geometry of the system whereas the particle scale physicochemical processes are treated in a simplified way reducing the computational effort but retaining the parametric dependency of the process. As a case study, one of the flocculation tanks of the water refinery of the city of Thessaloniki (Greece) is examined. It is shown that for the case of low solids concentration in the feed stream, flocculation is very weak to lead to particles large enough that can settle in the subsequent sedimentation tank. In this case, flocculation need be enhanced by increasing the solids concentration in the flocculation tank by recycling sludge from the sedimentation tank. Furthermore, guidelines are provided on how the present computational tool can be used for the optimization of the design and operation of flocculation tanks treating potable water from relatively clean sources.

1. Introduction

In modern water treatment technology, flocculation is a very important component of the overall suite of treatment processes. The need for a profound understanding and successful design/optimization of flocculation processes is more important today than in the past since the requirements for the removal of particulates have become increasingly stringent [1]. The complexity of the overall large scale flocculation process calls for its decomposition in two distinct conceptual components: The first refers to the floc scale physicochemical processes (floc scale hydrodynamics, flocculant adsorption dynamics, and collision rate). This scale can be studied experimentally using laboratory equipment with a well-defined flow field permitting the quantitative assessment of the involved processes. Unfortunately, information on this component alone does not suffice to describe the performance of large scale flocculation tanks. The second conceptual component refers to large scale tank hydrodynamics and its interaction with the local physicochemical processes. Both components are crucial and they must be taken into account in order to evaluate the overall large scale flocculation process.

The geometrical complexity of most flocculation tanks and the existence of moving parts make the solution of the governing equations for the macroscopic flow field a very difficult task. The basic assumption so far to make such a solution possible is that everything is well mixed in the tank and the turbulence intensity is uniformly distributed [1]. However, it is understood that this assumption has to be relaxed since turbulent intensity exhibits a very uneven distribution in the tank. An alternative approach often used in the past to relax this assumption [2,3] is the so-called compartmental modeling: the tank is divided in a finite number of well mixed regions each one with different but uniform properties. This approach permits a more detailed handling of the local physicochemical processes. The most recent approach based on the combination of the detailed floc-level treatment with the detailed treatment of the macroscopic flow field using a Computational Fluid Dynamics (CFD) code requires very high computational efforts. An appropriate approach to reduce the computational cost is not the simplification of the local scale problem by omitting physical parameters but the employment of special mathematical techniques to reduce the degrees of freedom of the corresponding population balance equation. The details of the geometry and of the operation of the flocculation tank are in most cases more important than the knowledge of the details of the floc size distribution. On this account, the extent of knowledge on the size distribution can be reduced mathematically in order to save computational power. It must be noted that the literature on CFD simulations of wastewater treatment is rather rich with cases where large mass fractions of solids lead to a two-way interaction between the liquid and

* Corresponding author. Tel.: +30 2310 997767; fax: +30 2310 99 7759.
E-mail addresses: ksamaras@chem.auth.gr (K. Samaras), zoubouli@chem.auth.gr (A. Zouboulis), karapant@chem.auth.gr (T. Karapantsios), kostoglu@chem.auth.gr (M. Kostoglou).

1385-8947/$ – see front matter © 2010 Elsevier B.V. All rights reserved.
doi:10.1016/j.cej.2010.05.032

Nomenclature

C	impeller clearance (distance from the tank bottom)
c	polymeric flocculant concentration
c^*	critical polymeric flocculant concentration
d	average diameter (corresponding to the average volume) of the fresh flocs
D	impeller diameter
$f(x)$	number density distribution of flocs
$g(x)$	number density distribution of mud particles
K	rate of effective collisions between flocs leading to permanent attachment
K_e	rate of encounters between flocs
M_f	volume fraction of fresh flocs
M_g	volume fraction of mud particles
N	total number concentration of fresh flocs
R_1, R_2	floc diameters
S	particle source
T_1	bottom tank diameter
T_2	top tank diameter
u	local velocity vector
x, y	floc volumes
x_o	average volume of fresh flocs

Greek symbols

α	collision efficiency
Γ	dispersion coefficient tensor
ε	turbulent energy dissipation rate
ν	kinematic viscosity of water

solid phase [4]. Yet, this is not so for the much simpler problem of CFD simulation for potable water treatment where the solids mass fraction is low.

The scope of the present work is not to advance the state of the art simulation tools based on CFD and/or population balances created for wastewater applications, but the development of an efficient computational tool for the simulation of flocculation tanks of a water refinery. A flocculation tank in Thessaloniki's (Greece) water refinery is used as a case study. This tool combined with the corresponding tool for sedimentation tanks will allow understanding the actual water clarification process and will set the basis for the optimization of the operational parameters of the process. The structure of the work is the following: First, the actual process is described in detail. Then the computational tool is described extensively starting from the CFD tool for the tank hydrodynamics and ending with the reduced population balance used for the computation of the local flocculation rates and the corresponding floc size evolution. Finally, several results of the simulation are presented and discussed extensively. The key point of the present modeling effort is to understand the dominant mechanism for the actual successful operation of the flocculation tank.

2. Problem statement

The refinery of Aliakmonas river water is the main water supplier of the metropolitan area of Thessaloniki and its suburbs. The maximum throughput of the refinery is 150,000 m^3/day. At present there are three identical flocculation/sedimentation (F/S) combined tanks in use, but an expansion to two more tanks is foreseen for the future.

At the refinery, the river water is subjected to a series of processes. After a pre-treatment (pre-ozonation, pH correction, and fast mixing), the water enters the main treatment processes (flocculation, sedimentation, filtration, ozonation, and activated carbon absorption), and finally undergoes chlorination and pH correction, in order to become suitable for consumption. It is very important to mention that an inorganic coagulant is continuously injected (aluminium sulfate) at the refinery's water mainstream shortly before it enters the F/S tanks. By doing that, the coagulation of particulates begins already before the mainstream enters the flocculation tank forming flocs of above 30 ± 5 μm mean size. The floc size is measured by a *Malvern–Mastersizer 2000* (diffraction light scattering device) and it is computed from several samples taken from the mainstream, before it enters the F/S tanks. In the same way, the floc size at the outlet of the flocculation tank (inlet of the sedimentation tank) was found to be at above 280 ± 35 μm (see [5] for a complete floc size distribution). The whole process operates at steady state so the exact sampling times are not of relevance since all measurements were performed at a period of constant conditions in the feed.

2.1. Technical details of the tank

As stated before, the refinery operates with three identical tanks for combined flocculation and sedimentation. The tanks have two concentric compartments of cylindrical shape: the inner flocculation tank and the outer sedimentation tank. The two compartments communicate with each other in two ways. There is a flow from the inner to the outer tank through an overflow perimetric channel whereas there is a flow, at the reverse direction, through four inclined tubes which recycle part of the mud accumulating at the bottom of the sedimentation tank (see Fig. 1). It is noted that the word *mud* is used in the present work instead of the usual terminology sludge. This is done deliberately in order to discriminate the concentrated sludge from its diluted form (consisting of sludge particles) which is called mud.

The flocculation tank is cylindrical along its height and becomes narrower at the upper section (see Fig. 1). The major geometric dimensions of the tank are:

- Tank diameter: $T_1 = 9.57$ m bottom–$T_2 = 7.56$ m at the top.
- Total height: $H = 5.65$ m.
- Impeller type: Mixel tt (down pumping).
- Impeller diameter: $D = 3.88$ m (ratio $D/T_1 = 0.4$).
- Impeller clearance (distance from bottom): $C = 2.8$ m (ratio $C/H = 0.5$).

The major operational parameters of the tank are:

- Agitation speed: 9 rpm ($V_{tip} = 1.83$ m/s).
- Water flow rate: 40,000 m^3/day = 462 kg/s (80% of maximum throughput).
- Mud flow rate: 4000 m^3/day = 46.2 kg/s.
- Polyelectrolyte flow rate: 1.16×10^{-3} kg/s.

The concentrations of the various ingredients at the input flow rates are:

- Small flocs concentration at the main tank feed stream: 2.4×10^{-4} kg/kg water.
- Flocs diameter at the main tank feed stream: 30 μm.
- Mud concentration at the recycling streams: 7×10^{-3} kg/kg water.
- Polyelectrolyte concentration at its feed stream: 5×10^{-4} kg/kg water.

2.2. Simulation of the flocculation tank

The flocculation tank is designed and simulated with the computer software *Ansys CFX*© [6], in a 1:1 scale. The design is very

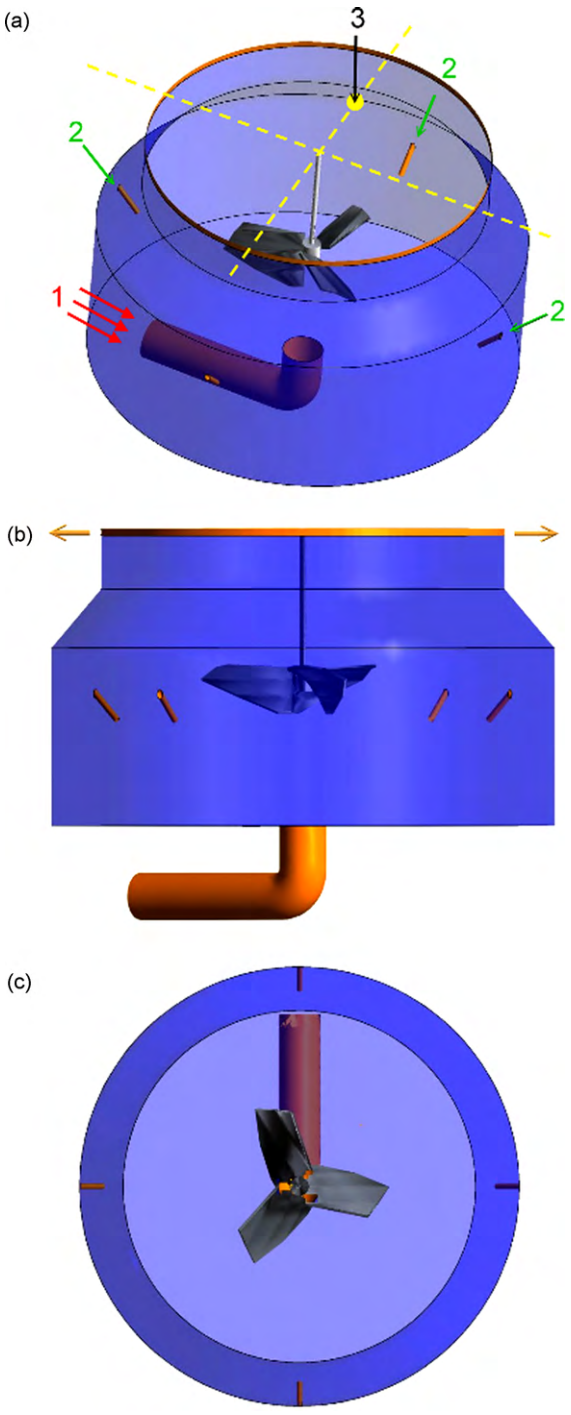

Fig. 1. Geometric points of view of the tank. (a) 3D perspective. Numbers indicate the three input streams: (1) water main feed, (2) mud recirculation, (3) flocculant feed. (b) Side view. The arrows at the top are pointing at the perimetric outflow to the sedimentation tank. (c) Top view.

accurate as it is based on actual geometrical and technical details that are made available from the blueprints of the company which operates the refinery. The computational grid of the tank is tetrahedral with multiple prismatic layers near the walls (Fig. 2). In total, approximately 825,000 cells are used, which corresponds to 210,000 computational nodes. A run performed using a denser grid has led to a much higher computational time with only a very small change of the average flow quantities which is totally acceptable for the scope of the present work.

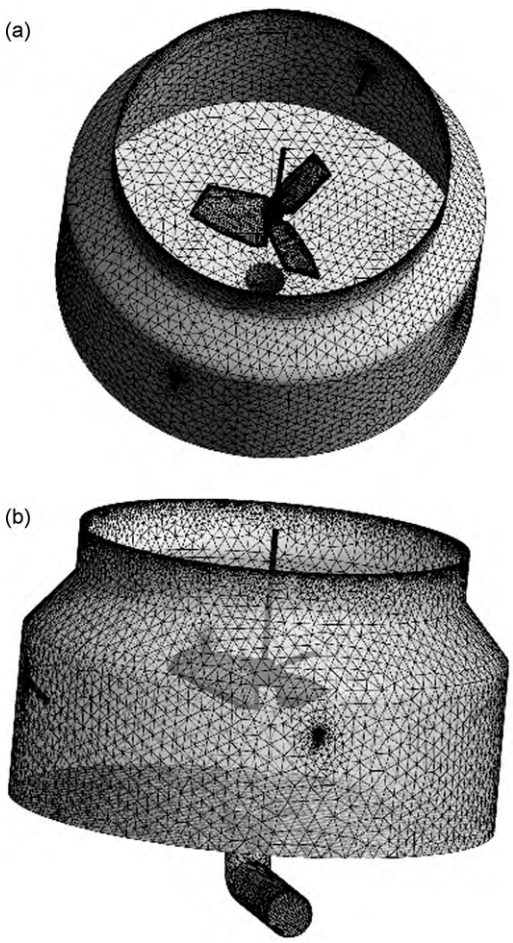

Fig. 2. Tetrahedral computational grid used for the simulation of the tank; two different 3D perspectives.

3. Problem solution

3.1. Single phase hydrodynamics

The estimation of the turbulent flow field in a stirred tank is by far no trivial and it has been the subject of intensive research during the last decades. The first step is typically the time averaging, in order to get the Reynolds Averaged Navier–Stokes (RANS) equations where the closure of the system is achieved by the appropriate k–ε model (a detailed review of turbulent models can be found in Wilcox [7]). The solution of the RANS is very difficult due to the moving computational domain imposed by the motion of the impeller that makes the problem inherently transient and three-dimensional.

An older computational approach to deal with the problem is to bypass the explicit handling of the impeller motion by dividing the flow field in two regions. The one region includes the impeller and it is not discretized at all. Experimental values of the variables on the external boundary of the impeller region are used as boundary condition for the solution of the RANS in the second region [8]. During the last decade, the advancement of computational techniques and the advent of computer power made possible the complete solution of the mathematical problem without the employment of experimental information. One technique to achieve this is based on sliding meshes [9]. A much simpler approach is the so-called multiple reference frame (MRF) technique [10]. The computational domain is divided again into two zones similar to the older experimental data based technique. The difference is that now the RANS

are solved also in the inner (impeller) region employing a reference frame, which follows the motion of the impeller. In this way the boundary conditions of the inner regions on the impeller can be immobilized and the transformed system of equations does not include explicitly the time. In the second zone (outer zone), the governing equations are discretized in the conventional stationary frame, relative to the tank walls. The equations in this second zone also do not include an explicit time dependence. The non-steadiness appears in the boundary conditions at the interface between the two zones where all the variables defined on the moving inner frame of reference must be transformed to variables defined on the outer stationary frame of reference [11]. The explicit appearance of time in the problem has to do with the change in the geometry and, correspondingly, in the flow field according to the instantaneous position of the impeller. So, in principle a flow field must be found for each phase angle of the impeller.

The real strength of the MRF technique appears when the dependence from the phase angle of the impeller can be ignored leading to a pseudo-steady state flow field (the term pseudo implies that the flow field "moves" with the impeller). This approximation is exact for the case of a purely cylindrical tank. In case of no-radial symmetry (e.g. due to baffles, non-cylindrical tank, side input/output streams) the success of approximation depends on the degree of interaction of the impeller motion with the elements that destroy the symmetry (in case of baffles the ratio of baffle width to tank radius determines the success of the steady state approximation). In the present work the radial symmetry requirement is violated due to the side feed streams in the tank. However, the computed flow fields indicate a very weak interaction between the local flow field at the stream entries and the impeller motion so the steady state approach can still be followed. In recent studies [12,13] a detailed comparison of CFD results based on several turbulence models with experimental data of fluid velocity for the case of a jar tester has been performed. Those results suggest the use of advanced turbulence models (e.g. Reynolds stresses) for a quantitative estimation of the velocity profile. On the other hand, some computationally efficient two equation models give acceptable results for the average ε value. Based on these results the Renormalized Group k–ε model is preferred in the present work against the standard k–ε model which gives quite wrong results for the case of flow fields created by impellers.

3.2. Treatment of the solid particles phase

In principle the mixture of water with solid particles should be treated as a two-phase flow mathematical problem. The simulation of the dispersed phase for volume fraction less than 10% can be Lagrangian (trajectory calculations for discrete particles) or Eulerian, whereas an Eulerian approach is always used for the continuous phase. In the Eulerian–Eulerian approach the two phases are treated as interpenetrating continua coexisting in the same space and the conservation equations are written separately for each phase including terms for the interaction between the phases [6]. In the present case although the volume fraction of the dispersed phase is very small the Lagrangian approach is not appropriate because it cannot handle the coagulation of flocs.

The particle mass loading in a sedimentation tank for potable water treatment is typically very small, and therefore, it can be safely assumed that the presence of the particles does not affect the flow field (one-way coupling). Furthermore, the gravitational settling of flocs in the flocculation tank can be neglected based on (a) its relatively small residence time, (b) the mixing imposed by the impeller and (c) the experimental observation that no particles settle in the actual flocculation tank. The size and density of flocs are such that their Stokes number is less than 1. The combination of the flocs small Stokes number and negligence of their settling velocity yields a particle phase following completely the motion of the continuous phase, which implies that there is no need to consider particles as a second phase. For this reason passive scalar description of the particle phase is very beneficial from the computational point of view since only the conservation and not the momentum equations need to be solved.

3.3. The coagulation problem

Let say that the size distribution of flocs can be described by the function $f(x)$ such as $f(x)dx$ is the number concentration of flocs with volume x. The function $f(x)$ at steady state depends on the position inside the tank and its spatial distribution is described by the equation:

$$u \cdot \nabla f = \nabla \cdot \Gamma \nabla f + S \tag{1}$$

where u is the local (Reynolds averaged) velocity vector of the fluid phase, Γ is the turbulent dispersion coefficient (result of the turbulent velocity fluctuations) and S is a source term. In the present work, the flocs breakage will be ignored since the turbulent intensities are relatively low (slow rotation of the impeller) so the source term S includes only the contribution from the flocs coagulation phenomenon (this assumption will be further discussed below). Specifically, the coagulation source term has the form [14]:

$$S = \frac{1}{2}\int_0^x K(y, x-y)f(y)f(x-y)dy - f(x)\int_0^\infty K(x, y)f(y)dy \tag{2}$$

The function $K(x,y)$ is called coagulation kernel and gives the frequency of coagulation events between two flocs of size x and y, respectively. It is noted that in the derivation of (2) the usual approach for the source terms when modeling turbulence is employed, that is, the time average of the functions of instantaneous quantities is equal to the functions of the time averages of instantaneous quantities [15]. This approach is just an approximation for non-linear phenomena like coagulation and in fact a micromixing model should be employed instead [16]. But the relatively weak non-linearity of the coagulation terms (compared to that of nucleation for example) makes the above simplified approach acceptable for the level of sophistication employed in the present wok.

Flocs collide to each other due to the turbulent flow field in the tank. In principle, turbulence induces encounters between suspended particles in two distinct ways. Particles with size smaller than the smallest eddy of the flow field follow exactly the fluctuating local fluid velocity and this motion leads to encounters of first kind. The frequency of these encounters (turbulent mechanism) is given as

$$K_e(R_1, R_2) = 1.29(R_1 + R_2)^3\left(\frac{\varepsilon}{\nu}\right)^{1/2} \tag{3}$$

where ε is the turbulent energy dissipation rate and ν is the kinematic viscosity of the fluid. The above expression has been derived for the first time by Saffman and Turner [17]. Later, several other researchers used it with a different numerical constant in place of 1.29.

Particles of larger size (spanning several eddies) exhibit inertia with respect to turbulent flow fluctuations leading to a motion of particles different from that of the fluid. This motion constitutes the second mechanism of turbulent aggregation [18]. It can be confirmed by a simple calculation that for the particle size, particle densities and turbulence intensities of the present work this mechanism has no contribution to collision between particles.

Eq. (3) has been derived for spherical particles. In the present study this assumption is retained for the shape of the flocs. More sophisticated flocculation models have been developed in

literature assuming flocs as fractal objects and employing the corresponding mass–radius relation in Eq. (3) [19]. In even more sophisticated models the fractal dimension is itself a dynamic variable evolving during the flocculation process [20,21]. Another important point is that Eq. (3) refers to all encounters between the flocs. However, only some of the encounters are actually effective leading to permanent attachment and this is expressed by the introduction of the collision efficiency α ($0 < \alpha \leq 1$):

$$K(R_1, R_2) = \alpha K_e(R_1, R_2) \tag{4}$$

The purpose of using a polymeric flocculant is to increase the collision efficiency α, which is a function of the adsorbed polymer quantity on a floc [4]. So, in principle a conservation equation similar to Eq. (1) must be written for the polymer with appropriate source terms to account for sorption–desorption to flocs. Furthermore, an additional independent coordinate must be introduced accounting for the amount of polymer adsorbed on each floc. Additional complications arise from the fact that the polymer is deactivated during the process due to scission [4]. The complete problem is extremely complicated so in the absence of specific data on the flocculant adsorption dynamics and trying to keep the sophistication of the model at engineering design levels the following assumptions are made: (a) The polymer adsorption–desorption kinetics is extremely fast compared to the flocculation kinetics so the amount adsorbed on the flocs is always in equilibrium with the local liquid phase concentration. (b) The equilibrium is shifted to the liquid phase, which means that the adsorbed polymer corresponds to a small amount of the total polymer, which means that the source term in the polymer conservation equation can be ignored. Based on the above assumptions and assuming a typical exponential dependence between the collision efficiency and adsorbed polymer yields:

$$\alpha = 1 - e^{-c/c^*} \tag{5}$$

where c is the liquid phase concentration of the polymer and c^* a critical polymer concentration. A step function has been employed by [4] instead of the smoother exponential one (but without the assumption of fast adsorption).

The coagulation term must be treated appropriately in order to replace the integrodifferential population balance equation with a system of discrete scalar equations which must be solved by the CFD code. One way to achieve this is to divide the particle size domain in classes. All the flocs belonging in a class are assumed to have the characteristic size of the class [22]. The unknowns in this method are the concentrations of particles in each size class leading to many degrees of freedom and making the use of this method cumbersome for 3D realistic geometry simulations. An alternative method with fewer degrees of freedom is the so-called method of moments [23,24]. According to this approach a particular shape of the $f(x)$ is assumed and the unknowns are the parameters of this shape. Here an approach of this type will be used.

The boundary conditions of the mass conservation equation are the particle size distribution in the main inlet flow stream and in the recirculation stream. Recognizing the importance of particles of the recirculation stream on the flocculation process and based on their different nature (with respect to the main flow stream particles), they are treated as a separate population described by the function $g(x)$. Therefore separate population balance equations need be written for the two functions $g(x)$ and $f(x)$. This makes the solution of the mathematical problem even more difficult. The main rational assumption at this point is that f particles are much smaller than g particles so the f particles contribution in the coagulation frequency between f and g particles can be ignored. This assumption can be justified by the measured and computed floc sizes. That is, the g particle size is about 280 μm (measured particles at the outlet of flocculation tank) whereas the f particle size is in most cases smaller than 100 μm (estimated from the simulations). Employing the simplest of the methods of moments, the so-called monodisperse approximation (which have been proved useful for engineering calculations [25]) the function f can be approximated as $f(x) = N\delta(x - x_o)$ where δ is the Dirac delta function, N is the total *fresh* particles number concentration, x_o is the average volume of these particles defined as $= M_f/N$ where M_f is their total volume concentration (volume fraction). The corresponding volume fraction of the mud particles is denoted M_g and it is the only needed quantity related to $g(x)$. Substituting the relation for $f(x)$ into the populations balance equations and taking the integral with respect to x (directly or weighted by x) from $x = 0$ to ∞ yields the following equations (only the source term is given):

$$\text{Equation for N}: S = -\frac{1}{2}\left(1.29 \cdot \frac{6}{\pi}\right)\alpha M_f N\left(\frac{\varepsilon}{\nu}\right)^{1/2} - \left(1.29 \cdot \frac{6}{\pi}\right)\alpha M_g N\left(\frac{\varepsilon}{\nu}\right)^{1/2} \tag{6}$$

The first terms refers to the loss of number of fresh particles due to coagulation between fresh particles and the second term due to coagulation with the mud particles.

$$\text{Equation for } M_f: S = -\left(1.29 \cdot \frac{3}{4\pi}\right)\alpha M_g M_f\left(\frac{\varepsilon}{\nu}\right)^{1/2} \tag{7}$$

The main reduction of fresh particles is due to their attachment onto mud particles. Fortunately, the only variable appearing in the equation for the description of mud particles is their total volume concentration which is increased due to scavenging by fresh particles. So:

$$\text{Equation for } M_g: S = \left(1.29 \cdot \frac{3}{4\pi}\right)\alpha M_g M_f\left(\frac{\varepsilon}{\nu}\right)^{1/2} \tag{8}$$

The final mathematical problem which must be solved includes only three scalars for the description of all particles in the system. This impressive reduction of the degrees of freedom was achieved using purely mathematical and not physical approximations retaining the parameters dependence on the physicochemical system and process operation. To achieve a high computational efficiency of the model the only sacrificed information is the detail of the size distribution. However, for engineering optimization process (based on a crude estimation of sedimentation) this information is much less important than the geometrical details of the process examined by the present model. At a second stage of the optimization procedure (having selected geometric details), a more detailed particle model capable of predicting particle size distribution is needed for the accurate computation of sedimentation efficiency.

4. Results and discussion

The base conditions under which the simulations are performed are that of the typical operation of the unit given in Section 2. Only the parameters with value different from the base case will be mentioned explicitly. It is found very convenient to solve first the purely hydrodynamic problem until achieving convergence and then to start iterations of the particle conservation equations. When stirring the particular tank with the mixel tt impeller the velocity flow field is as shown in Fig. 3. As stated before, this impeller is axial and more specifically down pumping. This means that the impeller creates a stream that heads to the bottom and so counterflows with the up-coming water inlet mainstream. From the two counteracting streams the inlet water mainstream prevails. At the tip of the impeller some small vortices are created, a characteristic attributed to the employed tip speed.

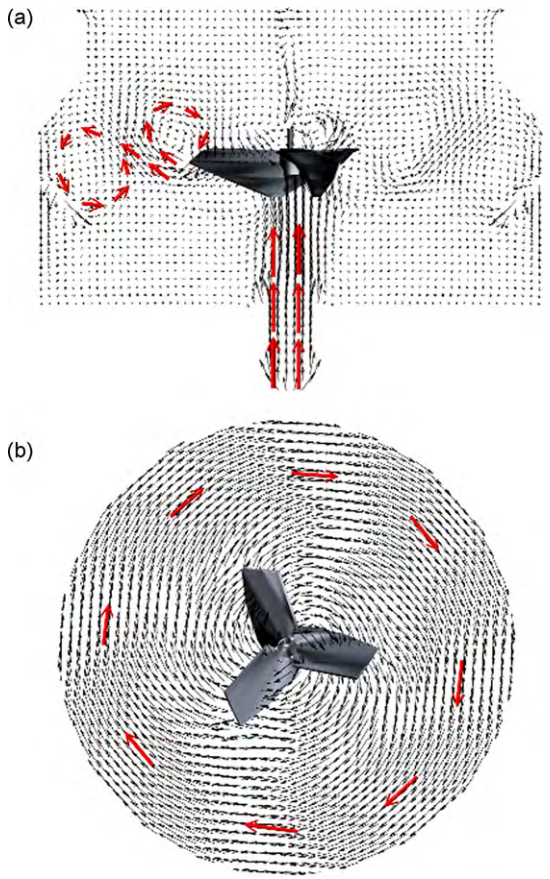

Fig. 3. Velocity flow field (water) for agitation speed of 9 rpm. (a) Side view at the plane of the impeller rotation axis, showing with arrows the upward inlet main feed and the two small vortices, created by the impeller tip. (b) Top view at the impeller elevation, showing a typical mixing profile.

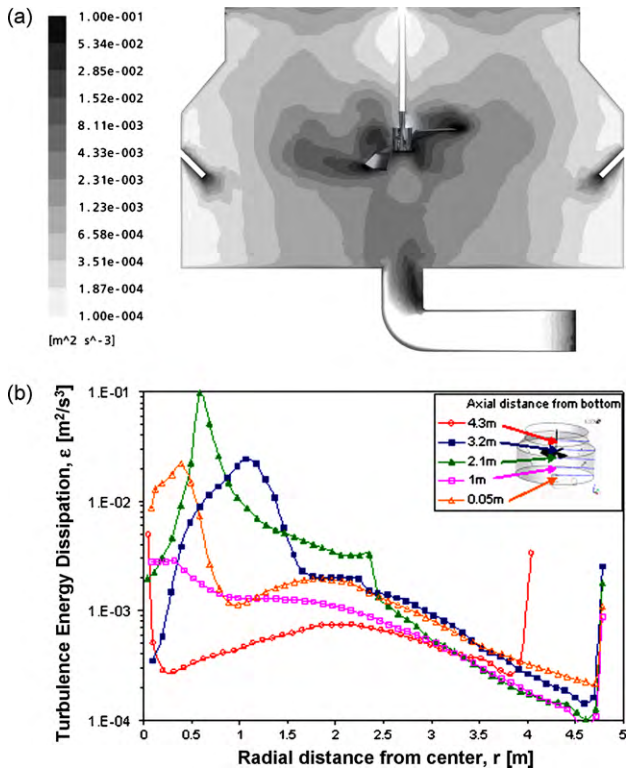

Fig. 4. (a) Vertical map of the distribution contours of the turbulent energy dissipation ε, (b) turbulent energy dissipation rate ε along tank radius at several heights (shown in the inset).

The distribution of the turbulent energy dissipation rate ε in the tank is shown in Fig. 4(a). It is evident that this distribution is highly non-uniform showing a maximum value close to the impeller tip and decreasing towards the walls of the tank except at the regions of the inlet flows where a local increase is observed. The high non-uniformity of ε distribution makes the usual field engineering approach of considering an average ε throughout the tank questionable and underlines the importance of a detailed system geometry consideration. To get a better idea of the non-uniformity of the ε distribution in the tank curves of ε values along tank radius at a particular azimuthal direction and at several heights are shown in Fig. 4(b). The ε axis is in logarithmic scale revealing the extreme non-uniformity of ε. As it is shown, ε increases close to the solid surface (tank walls or impeller) even by two orders of magnitude. At this point it is stressed that typically the design of flocculation tanks for practical use is based on the distribution of ε (or equivalently of the mean shear rate) in the tank [26]. In the other limit, the complete population balance is solved in research-oriented studies focusing on aggregates properties [20]. The present suggestion for avoiding the computational cost of handling simultaneously hydrodynamic and physicochemical aspects is to decompose the problem to two components: (i) advanced hydrodynamics with simple physicochemistry and (ii) simple hydrodynamics with advanced physicochemistry. In the present case, the focus is on the first component.

All the results about the floc concentration are presented as mass fraction (in accordance with the inlet data) but in Eqs. (6)–(8) volume fractions appear. So a procedure is needed to relate volume to mass fractions. This can be done using the relation (volume fraction) = (mass fraction × water density)/(solid fraction of the floc × solid density) which is a valid approximation for low floc concentration. The solid fraction of flocs is computed using the effective floc density 1.066 kg/m^3 found in previous works [5,27] by comparing experimental and theoretical sedimentation rates from the sedimentation tanks of the particular water refinery, and an assumed intrinsic solid density equal to 2 kg/m^3. This leads to a solid volume fraction of flocs equal to 0.066.

Let us first see how each species (fresh particles, mud particles and polyelectrolyte) is distributed in the tank in steady state in the absence of coagulation (which means that for the first two species polyelectrolyte is absent) (Case I). The steady state distribution of the mass concentration of fresh particles in the tank is shown in Fig. 5. As it is expected in the absence of the flocculant only a small dilution is observed which is due to the sludge recirculation side streams. Correspondingly, a much stronger dilution is observed for

Fig. 5. Case I: Vertical map of the contours of fresh particles concentration [kg/kg water], in the absence of mud particles and polyelectrolyte. The floc concentration entering with the water mainstream at the bottom of the tank is 2.4×10^{-4} kg/kg water.

Fig. 6. Case I: Vertical map of the contours of mud particles concentration [kg/kg water], in the absence of coagulation. 7×10^{-3} kg/kg water is the mud concentration at the entrance of the recycling streams.

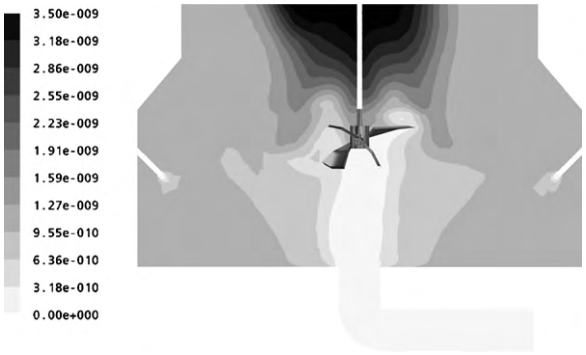

Fig. 7. Case I: Vertical map of the contours of polyelectrolyte concentration [kg/kg water], in the absence of coagulation. 5×10^{-4} kg/kg water is the concentration of the polyelectrolyte at its corresponding inlet.

the mud particles due to the lower sludge flow rate compared to the main inlet stream flow rate. As it is shown in Fig. 6 there is a zone free of mud particles in the trajectory of the main inlet stream and around the impeller. The concentration distribution of flocculant in the tank in steady state is presented in Fig. 7. According to this figure there are three distinct areas with respect to flocculant concentration: (a) a flocculant accumulation zone at the upper middle of the tank; (b) a flocculant free zone in the trajectory of the main inlet flow stream and (c) the rest of the tank in which the flocculant is distributed almost uniformly. Apparently, the flocculant distribution and utilization can be improved by changing the position of its entry. For example, it would be better to inject the flocculant close to the impeller or somewhere along the trajectory of the main inlet flow stream. This is not for achieving a better distribution of flocculant throughout the tank (improved mixing efficiency) but for having it available exactly at the region where it is needed (i.e. in the impeller zone).

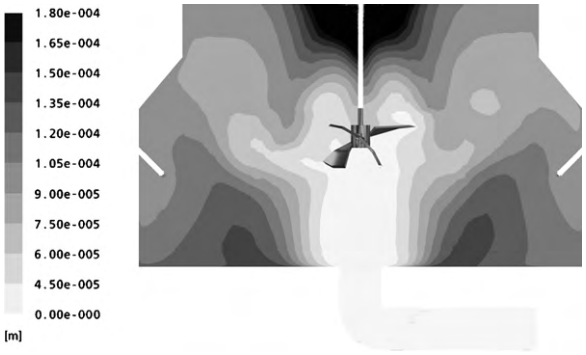

Fig. 8. Case II: Vertical, contour map of the mean flocs diameter.

Fig. 9. Case III: Vertical map of the contours of fresh particles concentration [kg/kg water].

Fig. 10. Case III: Vertical map of the contours of mud particles concentration [kg/kg water].

Next, we investigate what happens in the tank in the presence of fresh particles and flocculant (no mud stream particles) (Case II). In this case, coagulation among fresh particles occurs in a rate depending both on the local flocculant concentration and the local energy dissipation rate. The mass concentration distribution of fresh particles is exactly the same with the one shown in Fig. 5 since coagulation is a mass preserving phenomenon. The spatial distribution average volume equivalent diameter $d\,(=\pi/6(M_f/N)^{1/3})$ of flocs is shown in Fig. 8. It is surprising that there are no large flocs in the region close to the impeller (given that breakage is not considered). The flocs actually grow in regions of high residence time (such as the region of the accumulation of flocculant) but these regions hardly contribute to the floc size in the peripheral outflow to the sedimentation tank. The size of the resulting flocs (average diameter 97 μm but the complete distribution includes also smaller particles) is not large enough to ensure acceptable sedimentation efficiency. The difference between the particular process examined here and processes in which flocculation leads to efficient sedi-

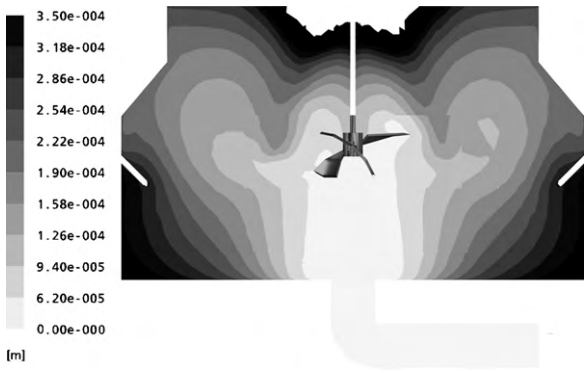

Fig. 11. Case IV: Vertical, contour map of the mean flocs diameter.

Table 1
Mean values over the whole volume of the tank and at the peripheral outlet of the 'fresh flocs', the 'mud' and the mean floc diameter for all the 6 cases studied.

Case	'Fresh' flocs (kg/kg water)		'Mud' (kg/kg water)		Average fresh floc diameter (μm)	
	Tank	Outlet	Tank	Outlet	Tank	Outlet
I	2.17×10^{-4}	2.19×10^{-4}	6.94×10^{-4}	6.27×10^{-4}	30	30
II	2.17×10^{-4}	2.19×10^{-4}	6.94×10^{-4}	6.27×10^{-4}	109	97
III	3.78×10^{-6}	4.14×10^{-9}	9.18×10^{-4}	8.45×10^{-4}	32	32
IV	2.20×10^{-4}	2.20×10^{-4}	6.65×10^{-4}	5.92×10^{-4}	231	216
V	2.90×10^{-6}	1.88×10^{-13}	9.28×10^{-4}	8.09×10^{-4}	30	30
VI	4.40×10^{-6}	4.46×10^{-8}	5.83×10^{-4}	5.38×10^{-4}	32	32

mentation is the very low concentration of solids in the present case. Coagulation depends on solids concentration (in addition to turbulence level) and although it can be effective for applications with high solids content (waste water treatment, activated sludge removal) this is not so when handling the relatively clean water of the present application.

Next, we examine the influence of mud recirculation on the flocculation process (Case III). The main action of mud particles is to increase the local solid fraction resulting in higher coagulation rates between mud and fresh particles. In this way, mud particles act as a sink for fresh particles leading to the reduction of their concentration. The mass concentration distribution of fresh particles is shown in Fig. 9. Only a small fraction of fresh particles leaves the tank as small fresh particles; the rest leave the tank as part of large mud particles. The distribution of the mass concentration of mud particles is shown in Fig. 10. The concentration of these particles increases in the tank due to the *adsorption* of the smaller fresh particles. The size of fresh particles is much smaller than in the case without mud particles. This is expected since the reduction of the fresh particle concentration due to their adsorption by the mud particles leads to negligibly smaller coagulation rates among fresh particles. The large mud particles further augmented by the amount of fresh particles attached on them will settle down in the sedimentation tank and only the free fresh particles will elude settling. This means that the present potable water purification process is very different than the usual flocculation–sedimentation set up. The sedimentation efficiency is not determined here by the growth of the incoming particles but from the amount of these particles that have coagulated with large mud particles that have been recirculated from those settled in the sedimentation tank. Of course, issues such the start-up and the overall dynamics of this process are not trivial and their study requires a higher level of description of the particulate phase (complete particle size distributions).

The negligence of the breakage phenomenon is confirmed by the results of the present work. Regarding fresh particles, their size is found always less than 100 μm. For this size and the average shear rate in the tank, 30 s^{-1}, computed from CFD results, it appears that according to experimental data in literature the effect of breakage is negligible [27,28]. Regarding mud particles the only assumption needed is that they are larger than fresh particles so the question of existence of breakage is irrelevant for the particular model.

In order to show how the computational model developed here can be used to better understand and optimize the process, three additional simulations with different values of the main operating parameters are presented. The first one (Case IV) is similar to Case II (no mud/fresh particles collision) but the stirring velocity is double (18 rpm). The second one (Case V) includes all the collision modes and also the double stirring velocity and the third one (Case VI) includes all the collision modes, the base case stirring velocity (9 rpm) and half the flow rate of the recirculation stream (i.e. 23.1 kg/s). The distribution of the average floc diameter in the tank for Case IV is presented in Fig. 11. It is evident that the extent of coagulation is radically increased due to the higher turbulent energy dissipation produced by the higher stirring velocity. The outflow average size $d = 216$ μm ensures a good sedimentation efficiency [5]. It is noted that the floc size is overestimated in this case because (i) the value of ε is much lower than in Case II. For conventional stirrers the breakage frequency is proportional to stirring velocity to a power ranging from 2 (theoretical inertia subrange breakage [29]) to 2.4 (from experimental data of [30]). (ii) Breakage rate is a power law of particle size. According to the above, the breakage rate in Case IV is increased by almost an order of magnitude and the no breakage assumption may not hold anymore. In addition, the assumption for the relative sizes of f and g particles is under question in this case. Table 1 summarizes the results of all the simulations performed in the present study. In particular, for each one of the Cases I to VI the mass fraction of the fresh flocs, the mud flocs, and the average fresh floc diameter are given. In addition to the outflow stream averages, tank volume averages are given from the above quantities. These volume averages are indicative of how a quantity is distributed in the tank. The results of Case V show that the increase of stirring velocity increases more the rate of fresh-mud flocs collisions and the remaining fresh flocs are in so small concentration that correspond to a zero extent of coagulation among them.

In case the sludge recirculation stream flow rate is reduced to half of the base value (Case VI) this leads to a reduction of the removal efficiency from 0.999 to 0.99. If the new efficiency is still acceptable from the practical point of view, then the operational recirculation rate can be kept low since this leads to a significant amount of energy saving. This is a characteristic example of how tools like the one developed here can be employed to optimize water treatment units operation.

5. Conclusions

In the present work, a flocculation tank of the water treatment unit of Thessaloniki (Greece) is simulated. A special simulation approach is developed which while retaining the complete parametric dependence of the physicochemical problem it sacrifices the details of particle size distribution in order to gain computational efficiency. This computational efficiency permits the detailed simulation and analysis of the large scale hydrodynamics due to the geometry of the process. It was found that the examined flocculation tank does not operate in the usual mode found in other relevant processes (flocculation of feed particles) due to the low concentration of particles in the feed. The size rise of feed particles enabling their subsequent sedimentation in the adjacent sedimentation tank is achieved solely thanks to their attachment to larger particles entering the tank by recirculating the deposited sludge from the sedimentation tank.

The very efficient computational tool developed here can be used for the design and optimization of the geometric (impeller type, position of inlet streams) and operational (recirculation flow rate, impeller rotation frequency, flocculant amount) characteris-

tics of the process. As a spin-off of the present work, several issues of general scientific and technical interest emerge. The most important is that the flocculation procedure can be successful in creating aggregates large enough to sediment in the subsequent sedimentation step only if the concentration of solids in the feed stream is large enough. If this is not the case, other means must be employed (i.e. recirculation of a stream with high solids concentration) to ensure the appropriate concentration of solids in the flocculation tank. The whole process is very complex and it has not been studied until now since the study of flocculation tanks is restricted to their hydrodynamics and the few published works having taken into account the particle dynamics refer to simple tanks without the need for recirculation. The present work serves as a diagnostic tool for an existing flocculation tank focusing on its hydrodynamics but it is hoped that in the future the dynamics of flocculation tanks with recirculation will be studied in detail using advanced physicochemical models.

Acknowledgments

Thanks are due to the scientific personnel of the plant A. Papaioannou (Chem. Eng.), A. Samaras (Mech. Eng.) and M. Papagianni (Chem.), as well as to the EYATh (Organisation for Drinking Water Supply and Wastewater Treatment of Thessaloniki), owner of the plant, for their help in many ways.

References

[1] J. Bratby, Coagulation and Flocculation in Water and Wastewater Treatment, IWA Publishing, London, 2006.
[2] P.T.L. Koh, J.R.G. Andrews, P.H.T. Uhlherr, Flocculation in stirred tanks, Chem. Eng. Sci. 39 (1983) 975–985.
[3] P.T.L. Koh, J.R.G. Andrews, P.H.T. Uhlherr, Modeling shear-flocculation by population balances, Chem. Eng. Sci. 42 (1987) 353–362.
[4] A.R. Heath, P.T.L. Koh, Combined population balance and CFD modeling of particle aggregation by polymeric flocculant, in: Proceedings of the 3rd International Conference on CFD in the Minerals and Process Industries, CSIRO, Melbourne, Australia, December 2003.
[5] A. Goula, M. Kostoglou, T. Karapantsios, A. Zouboulis, A CFD methodology for the design of sedimentation tanks in potable water treatment. Case study: the influence of a feed flow control baffle, Chem. Eng. J. 140 (2008) 110–121.
[6] ANSYS CFX-Solver, Release 10.0: Theory and Modelling, Electronic Manual, SAS IP, Inc, 2004.
[7] D.C. Wilcox, Turbulence Modeling for CFD, second ed., DCW Industries Inc, California, 1998.
[8] A.D. Gosman, C. Lekakou, S. Politis, R.I. Issa, M.K. Looney, Multidimensional modeling of turbulent two-phase flows in stirred vessels, AIChE J. 38 (1992) 1946–1956.
[9] V.V. Ranade, D. Choudhury, Modeling of flow in stirred vessels: comparison of snapshot, multiple reference frame and sliding mesh approaches, in: 16th Biennial North American Mixing Conference, June, 1997.
[10] L. Oshimowo, Z. Jaworski, N.K. Dyster, E. Marshall, W.N. Nienow, Predicting the tangential velocity field in stirred tanks using the MRF model with validation by LDA measurements, in: 10th European Conference on Mixing, Delft, Netherlands, July 2000.
[11] D. Dakshinamoorthy, J.F. Louvar, Hotspot distribution while shortstopping runaway reactions demonstrate the need for CFD models, Chem. Eng. Commun. 193 (2006) 537–547.
[12] J. Bridgeman, B. Jefferson, S.A. Parsons, Computational fluid dynamics modelling of flocculation in water treatment: a review, Eng. Appl. Comput. Fluid Mech. 3 (2) (2009) 220–241.
[13] J. Bridgeman, B. Jefferson, S.A. Parsons, The development and application of CFD models for water treatment flocculators, Adv. Eng. Soft. 41 (2010) 99–109.
[14] D. Ramkrishna, Population Balances: Theory and Application to Particulate Systems in Engineering, Academic Press, San Diego, 2000.
[15] J. Baldyga, J.R. Bourne, Turbulent Mixing and Chemical Reactions, Wiley, New York, 1999.
[16] S. Rigopoulos, PDF method for population balance in turbulent reactive flow, Chem. Eng. Sci. 62 (23) (2007) 6865–6878.
[17] P.G. Saffman, J.S. Turner, On the collision of drops in turbulent clouds, J. Fluid Mech. 1 (1956) 16–30.
[18] J. Abrahamson, Collision rates of small particles in a vigorously turbulent fluid, Chem. Eng. Sci. 30 (1975) 1371–1379.
[19] J. Kim, T.A. Kramer, Improved orthokinetic coagulation model for fractal colloids: aggregation and breakup, Chem. Eng. Sci. 61 (1) (2006) 45–53.
[20] C. Selomulya, G. Bushell, R. Amal, T.D. Waite, Understanding the role of restructuring in flocculation: the application of a population balance model, Chem. Eng. Sci. 58 (2003) 327–338.
[21] M. Kostoglou, A.G. Konstandopoulos, S.K. Friedlander, Bivariate population dynamics simulation of fractal aerosol aggregate coagulation and restructuring, J. Aerosol Sci. 37 (2006) 1102–1115.
[22] M. Kostoglou, Extended cell average technique for the solution of coagulation equation, J. Colloid Interface Sci. 306 (2007) 72–81.
[23] M. Kostoglou, A.J. Karabelas, Comprehensive modeling of precipitation and fouling in turbulent pipe flow, Ind. Eng. Chem. Res. 37 (1998) 1536–1550.
[24] D.L. Marchisio, R.D. Vigil, R.O. Fox, Implementation of the quadrature method of moments in CFD codes for aggregation-breakage problems, Chem. Eng. Sci. 58 (15) (2003) 3337–3351.
[25] M. Kostoglou, A.J. Karabelas, On the breakage of liquid–liquid dispersions in turbulent pipe flow: spatial patterns of breakage intensity, Ind. Eng. Chem. Res. 46 (2007) 8220–8228.
[26] Y. Cho, S. Yoo, Y. Hwang, J. Roh, P. Yoo, C. Kim, Evaluation of the buffing volume in last third flocculation basin using CFD, Korean J. Chem. Eng. 27 (2) (2010) 511–517.
[27] A.M. Goula, M. Kostoglou, T.D. Karapantsios, A.I. Zouboulis, The effect of influent temperature variations in a sedimentation tank for potable water treatment—a computational fluid dynamics study, Water Res. 42 (13) (2008) 3405–3414.
[28] J.C. Flesch, P.T. Spicer, S.E. Pratsinis, Laminar and turbulent shear-induced flocculation of fractal aggregates, Mater. Interfaces Electrochem. Phenom. 45 (5) (1999) 1114–1124.
[29] J. Bridgeman, B. Jefferson, S.A. Parsons, Assessing floc strength using CFD to improve organics removal, Chem. Eng. Res. Des. 86 (8) (2008) 941–950.
[30] P.T. Spicer, S.E. Pratsinis, Coagulation and fragmentation: universal steady-state particle-size distribution, AIChE J. 42 (6) (1996) 1612–1620.